Crystallization of Sodium−Birnessite and Accompanied Phase Transformation

Jian Luo,[†] Aimin Huang,[†] Ssang Hyun Park,[†] Steven L. Suib,*[,†,‡] and Chi-Lin O'Young*[,§]

Department of Chemistry, Box U-60, and Department of Chemical Engineering and Institute of Materials Science, University of Connecticut, Storrs, Connecticut 06269-4060, and Texaco Research Center, Texaco, Inc., P.O. Box 509, New York 12508

Received November 13, 1997. Revised Manuscript Received April 9, 1998

X-ray diffraction (XRD), infrared (IR), and scanning electron microscopy (SEM) techniques have been used to monitor the crystallization of birnessite ($Na_4Mn_{14}O_{27}\cdot 9H_2O$, JCPDS card 32-1128) by aging MnO_x, which was produced from the oxidation of $Mn(OH)_2$ by $KMnO_4$ in an NaOH solution in the presence of Mg^{2+}. The crystallization process of birnessite can be divided into three stages: an induction period, a fast crystallization period, and a steady-state period. The crystallization of birnessite was accompanied by the crystallization and phase transformation of feitknechtite (β-MnOOH, JCPDS card 18-0804). Increasing the temperature will reduce the induction period and accelerate the crystallization and phase transformation. Increasing the basicity has almost the same effect as increasing the aging temperature. The crystallization process is also influenced by varying the molar ratio of MnO_4^-/Mn^{2+}. A diagram of produced phases at room temperature at different basicities and ratios of MnO_4^-/Mn^{2+} is obtained. The interconversion between birnessite and buserite ($Na_4Mn_{14}O_{27}\cdot 21H_2O$, JCPDS card 23-1046) is also discussed.

I. Introduction

In recent years the preparation and application of certain classes of octahedral molecular sieves (OMS) containing MnO_6 units have garnered a great deal of attention. Among these, the synthetic counterpart of todorokite, which has one-dimensional tunnels consisting of 3 × 3 MnO_6 units,[1,2] is especially interesting. Many papers have been published on its occurrence, syntheses,[3,4,10−12,34,35] characterization,[4,12,31] ion-exchange properties,[14,18] electrochemical properties,[5−9] and catalytic properties.[29−31] Its performance in acid−base catalysis, reduction−oxidation catalysis, and photocatalysis is also under extensive investigation.

Birnessite, a layered material with hydrated cations between the layers,[1,5−7,20−22] is an important precursor

* To whom correspondence should be addressed.
[†] Department of Chemistry, University of Connecticut.
[‡] Department of Chemical Engineering and Institute of Materials Science, University of Connecticut.
[§] Texaco Research Center.

(1) Bricker, O. *Am. Mineral.* **1965**, *50*, 1296−1354.
(2) Post, J. E.; Bish, D. L. *Am. Mineral.* **1988**, *73*, 861−869.
(3) Shen, Y. F.; Zerger, R. P.; DeGuzman, R. N.; Suib, S. L.; McCurdy, L.; Potter, D. I.; O'Young, C. L. *J. Chem. Soc., Chem. Commun.* **1992**, 1213−1214.
(4) Shen, Y. F.; Zerger, R. P.; DeGuzman, R. N.; Suib, S. L.; McCurdy, L.; Potter, D. I.; O'Young, C. L. *Science* **1993**, *260*, 511−515.
(5) Pereira-Ramos, J. P.; Badour, R.; Bach, S.; Baffier, N. *Solid State Ionics* **1992**, *701*, 3−56.
(6) Bach, S.; Pereira-Ramos, J. P.; Baffier, N. *Electrochim. Acta* **1993**, *38*, 1695−1700.
(7) Bach, S.; Pereira-Ramos, J. P.; Baffier, N. *J. Solid State Chem.* **1995**, *120*, 70−73.
(8) DeGuzman, R. N.; Shen, Y. F.; Shaw, B. R.; Suib, S. L.; O'Young, C. L. *Chem. Mater.* **1993**, *5*, 1395−1400.
(9) Bish, D. L.; Post, J. E. *Geol. Soc. Am. Abstr. Programs* **1984**, *16*, 625.
(10) Luo, J.; Suib, S. L. *J. Phys. Chem.* **1998**, submitted.
(11) Straczek, J. R.; Horen, A.; Warshaw, C. M. *Am. Mineral.* **1960**, *45*, 1174−1184.
(12) Golden, D. C.; Chen, C. C.; Dixon, J. B. *Science* **1986**, *231*, 717−719.
(13) Turner, S.; Siegel, M. D.; Buseck, P. R. *Nature* **1982**, *296*, 841−842.
(14) Burns, R. G.; Burns, V. M.; Stockman, H. *Am. Mineral.* **1983**, *68*, 972−980.
(15) Giovanoli, R. *Am. Mineral.* **1985**, *70*, 204−206.
(16) Giovanoli, R.; Burki, P. *Chimia* **1975**, *29*, 266−269.
(17) Mckenzie, R. M. *Mineral. Mag.* **1971**, *38*, 205−214.
(18) Feng, Q.; Kanoh, H.; Miyai, Y.; Ooi, K. *Chem. Mater.* **1995**, *7*, 1722−1727.
(19) Feitknecht, W.; Marti, W. Heiv. *Chim. Acta* **1945**, *28*, 129−148.
(20) Bach, S.; Henry, M.; Baffier, N.; Livage, J. *J. Solid State Chem.* **1990**, *88*, 325−333.
(21) Parent, J.; Olazcuaga, R.; Devalette, M.; Fouassier, C.; Hagenmuller, P. *J. Solid State Chem.* **1971**, *3*, 1−11.
(22) Buser, W.; Graf, P.; Feitknecht, W. *Helv. Chim. Acta.* **1954**, *37*, 2322−2323.
(23) Burns, R. G.; Burns, V. M. *Philos. Trans. R. Soc., London (A)* **1977**, *286*, 283−301.
(24) Chukhrov, F. V.; Gorshkov, A. I. *Trans. R. Soc. Edinburgh* **1981**, *72*, 195−200.
(25) Frondel, C.; Marvin, U.; Ito, J. *Am. Mineral.* **1960**, *45*, 871−875.
(26) Jones, L. H. P.; Milne, A. A. *Mineral. Mag.* **1956**, *31*, 283−288.
(27) Golden, D. C.; Chen, C. C.; Dixon, J. B. *Clays Clay Miner.* **1987**, *35*, 271−280.
(28) Golden, D. C.; Dixon, J. B.; Chen, C. C. *Clays Clay Miner.* **1986**, *34*, 511−520.
(29) Nitta, M. *Appl. Catal.* **1984,** *9*, 151−176.
(30) Wong, S. T.; Cheng, S. *Inorg. Chem.* **1992**, *31*, 1165−1172.
(31) Yin, Y. G.;, Xu, W. Q.; Shen, Y., F.; Suib, L. S. *Chem. Mater.* **1994**, *6*, 1803−1808.
(32) Luo, J.; Segal, S. R.; Wang, J. Y.; Tian, Z. R. *Proc. MRS, San Francisco* **1996**, 3−8.
(33) Giovanoli, R.; Stahli, E.; Feitknecht, W. *Helv. Chim. Acta.* **1970**, *53*, 209−220.
(34) Turner, S.; Buseck, P. R. *Science* **1981**, *212*, 1024−1027.
(35) Turner, S.; Buseck, P. R. *Science* **1979**, *203*, 456−458.

S0897-4756(97)00745-X CCC: $15.00
Published on Web 05/28/1998

to todorokite.[2,3,12,15,17,32] The crystalline quality of synthetic todorokite is therefore largely dependent on that of the originally crystallized birnessite. In addition, birnessite itself can also be a potential catalytic and ion-exchange material. Many papers have been reported on the natural occurrence and synthesis of birnessite.[1−3,5−7,10,15,20−28,33,36] However, to our knowledge, no reports have as yet been published with a detailed description of the crystallization and accompanying phase transformation.

In this work, the crystallization of birnessite and accompanying phase transformations have been investigated by XRD, IR, and SEM. A possible route and mechanism for the formation of birnessite from MnO_x gel (including phase transformations) is proposed.

II. Experimental Section

A. Preparation Procedure. A typical synthesis is as follows: a solution of 13.5 g of $MnSO_4 \cdot H_2O$ (or 19.8 g of $Mn(Ac)_2 \cdot 4H_2O$) and 3.95 g of $MgSO_4 \cdot 7H_2O$ (or 3.2 g of $Mg(Ac)_2 \cdot 4H_2O$) in 160 mL of deionized distilled water (DDW) is added slowly to a solution of 40 g of sodium hydroxide in 180 mL of DDW with vigorous agitation, to form pink gels of $Mn(OH)_2$. A solution of 5.1 g of $KMnO_4$ in 160 mL of DDW is then added slowly into the gel during vigorous agitation, to produce a black suspension of MnO_x, the volume of which is about 530 mL. This suspension is aged at room temperature and atmospheric pressure. The resultant products at different crystallization times are filtered and washed. The amount of NaOH and $KMnO_4$ can be varied on the basis of this recipe to change the basicity and the ratio of MnO_4^-/Mn^{2+}. The synthesis with sulfates is used for the study of the crystallization process, while that with acetates is used to study the effects of temperature, basicity, and the ratio of MnO_4^-/Mn^{2+}. Similar procedures were reported in our previous work.[3,4,10]

The concentration of $[OH^-]$ (mol/L) of the system is calculated using the moles of NaOH (M_1), moles of Mn^{2+} (M_2), and the volume of the mixture (V) from eq 1:

$$[OH^-] = (M_1 - 2M_2)V \quad (1)$$

B. X-ray Diffraction Experiments and Crystallization Rates. XRD experiments were conducted using a Scintag XDS 2000 diffractometer, using Cu Kα radiation, with a tube current of 40 mA and a tube voltage of 45 kV. For each determination, 10 drops of the sample slurry (all with the same sample-to-water ratio and therefore the same thickness) were placed on the sample glass slide. When dried in air, the sample formed a uniform thin film on the slide. The area of the sample is much larger than the area of the X-ray beam. A wet sample is dark black while a dried sample is gray. A color change is observed when the sample film is dried. A sample is defined as newly dried within 5 min of when the color change takes place, after which it is a fully dried sample. A sample produced at $t > 30$ days was usually much larger in size. It was crushed by a ultrasonic treatment at the slurry stage before being placed on the glass slide. All the XRD patterns were obtained under identical conditions. The areas (S_i) of the two peaks at 2θ of 12.5° (002) and 25° (212) was obtained from Scintag software. The sum (S_m) of the areas is approximately proportional to the amount of birnessite in a product (crystallinity). The crystallinity was assigned as 100% for the sample with the largest sum of peak intensities (S_m), thus giving the relative crystallinity of birnessite (X_i) in other products as expressed in eq 2:

$$X_i = (S_i/S_m) \times 100\% \quad (2)$$

The crystallinity of feitknechtite is estimated similarly from the peak area at 19.5°.

The variation of relative crystallinity with time is referred to as the crystallization curve. In this study it is found that there exists a linear segment, corresponding to a fast crystallization period in the crystallization curve of birnessite. The slope of this segment is defined as the crystallization rate.

C. IR and SEM Studies. Birnessite product was washed and dried at room temperature for IR studies. Diffuse reflectance IR spectra of the samples were taken on a Nicolet Magna-IR System 750 FT-IR spectrometer, using standard measurement procedures. For each spectrum, 200 scans were employed with a resolution of 4 cm^{-1}.

SEM photographs were taken on an AMRAY 1810 scanning electron microscope. Graphite dispersed in 2-propanol was smeared on a sample holder, forming a film of graphite matrix when the solvent was evaporated. A drop of a sample dispersed in 2-propanol was then added to the newly dried graphite matrix. When dried in air, the sample was uniformly distributed and coated slightly with the conductive matrix.

III. Results

A. Synthesis of Birnessite. The synthesis of birnessite using sulfates was done at room temperature and atmospheric pressure. Usually the synthesis procedures contain three steps: the formation of $Mn(OH)_2$, the oxidation of $Mn(OH)_2$ to a MnO_x suspension by $KMnO_4$, and the aging of the MnO_x suspension to form birnessite. The $Mn(OH)_2$ formed was a pale pink gel-like slurry. When $KMnO_4$ solution was added to $Mn(OH)_2$, a brownish suspension of MnO_x was produced. The suspension turned dark black in 3 days, became grayish black in about 6 days, and after 20 days is somewhat greenish gray. A reviewer has suggested that the green color should be due to the formation of manganate. However, the green color cannot be removed by repeated washing. This color change may not be due to Mn(VI), which is green and soluble.

B. Phases Existing in the Synthesis Process. Figure 1 shows the XRD patterns of the products at different aging time. Three different types of peaks were recognized. The broad peak at ca. 2θ of 37° disappeared in about 5 days, the two peaks at 2θ of 12.5° and 25° increased in intensity with increasing aging time, and the peak at 2θ of 19.5° is considerably narrower than the other peaks. The peak at 2θ of 19.5° increased at first, remained constant for some time, gradually decreased, and finally disappeared. The peaks at 2θ of 12.5° and 25° are due to birnessite. The peak at 2θ of 19.5° is due to feitknechtite, also known as β-MnOOH, a brownish solid which was reported by Feitknecht[37] and Bricker[1] to form from the oxidation of $Mn(OH)_2$ with the coproduction of hausmannite[1,19] (γ-Mn_3O_4, JCPDS card 24-0734). The very broad peak at 2θ of 37° is quite likely due to oxidized hausmannite. However, many other manganese oxides with MnO_6 units may have some XRD reflections in this region.

Upon complete addition of all the starting materials (aging time $t = 0$), the birnessite phase could immediately be detected (Figure 1a). However, the strongest peak at that time was at 2θ of 19.5°, showing that the main product at the beginning was feitknechtite.

(36) Ching, S.; Landrigan, J. A.; Jorgensen, M. L.; Duan, N.; Suib, S. L. *Chem. Mater.* **1995**, *7*, 1604−1606.

(37) Feitknecht, W.; Oswald, H. R. *Helv. Chim. Acta.* **1960**, *43*, 1947−1950.

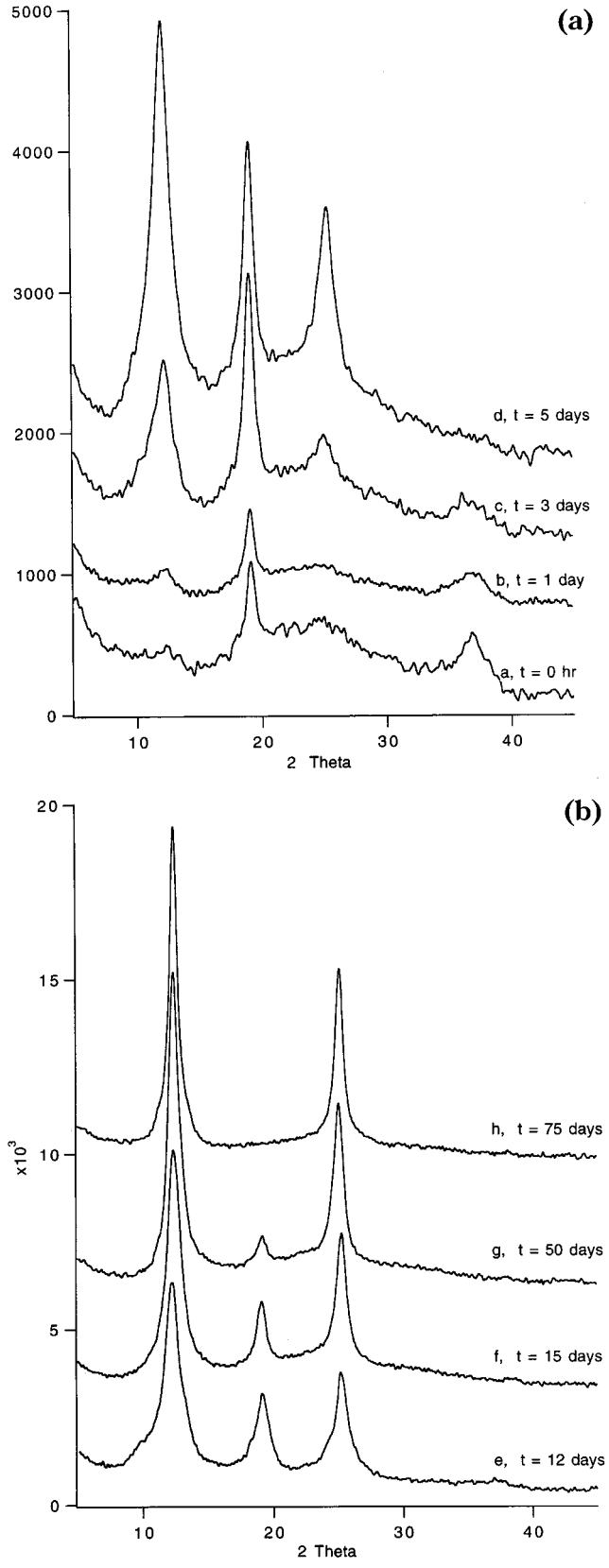

Figure 1. XRD patterns of birnessites at different crystallization times: t = (a) 0 days, (b) 1 day, (c) 3 days, (d) 5 days, (e) 12 days, (f) 15, days (g) 50 days, (h) 75 days.

Birnessite was only a minor phase at that time, and the amount changes very little in the following 32 h, after which the amount began to increase quickly. The early crystallization stage before the amount of birnessite increase rapidly is called an induction period hereafter.

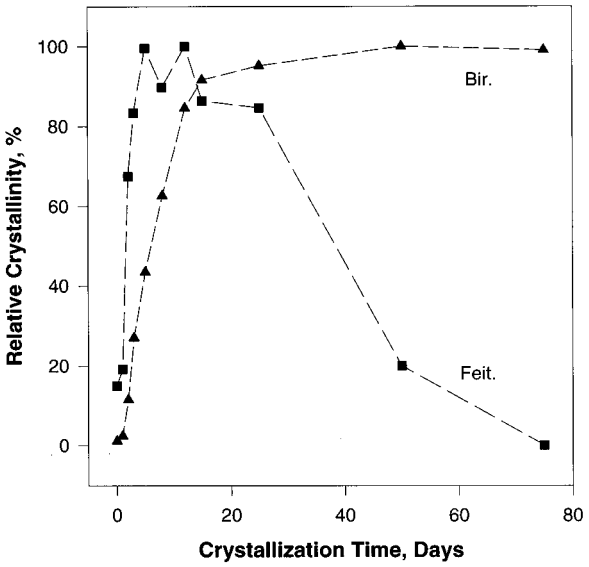

Figure 2. Crystallization curves of birnessites and feitknechtite.

The amount of feitknechtite phase increased slowly for some time (t = 5 days), did not change much from t = 5 days to 25 days, and after that began to decrease and finally disappeared in 75 days (Figures 1 and 2).

C. Crystallization Process Studied by IR. Figure 3 shows the IR spectra of samples after different crystallization times. Two very weak bands at ca. 460 and 510 cm^{-1}, which are characteristic IR absorptions of birnessite,[27,38] can be observed for samples at t = 0. The relative intensities of these two bands increased; i.e., the amount of total birnessite increased with crystallization time before t = 15 days, after which the amount of birnessite was substantially the same. Meanwhile, a peak at 670 cm^{-1} evolved and increased in intensity with increasing crystallization time.

All samples exhibited very strong absorption in the 4000−2500 cm^{-1} region, and were usually composed of several bands, as shown in Figure 3a. They are due to the IR absorption of interlayer hydrates and, possibly, some hydroxyl groups not from such hydrates but those directly bound to the interlayer metal ions. The broad band near 710 cm^{-1} is due to Mn−O. The band at 650 cm^{-1} could be due to Mn−O vibrations.

D. SEM Results. The early stage products have a very irregular morphology. At t = 0, the product was composed of ball-like particles of ca. 5 μm. In about 3 days the particles were changed to irregular sheets. Hexagonal platy crystals (ca. 10 μm for each side and a thickness of ca. 1 μm) can be found to evolve from the irregular sheets after 8 days. The morphology of birnessite is similar to that reported by Bricker,[1] except that the size in our work is much larger. Later, the crystals began to aggregate to larger masses (more than 100 μm), in which the crystals gradually lost their vertexes and prismatic appearances. After t = 90 days, the aggregates began to delaminate to form irregular platy products with a diameter of more than 100 μm (Figure 4).

E. Effect of Temperature, Basicity, and Ratio of MnO_4^-/Mn^{2+}. Table 1 shows the dependence of the

(38) Potter, R. M.; Rossman, G. R. *Am. Mineral.* **1979**, *64*, 1199−1218.

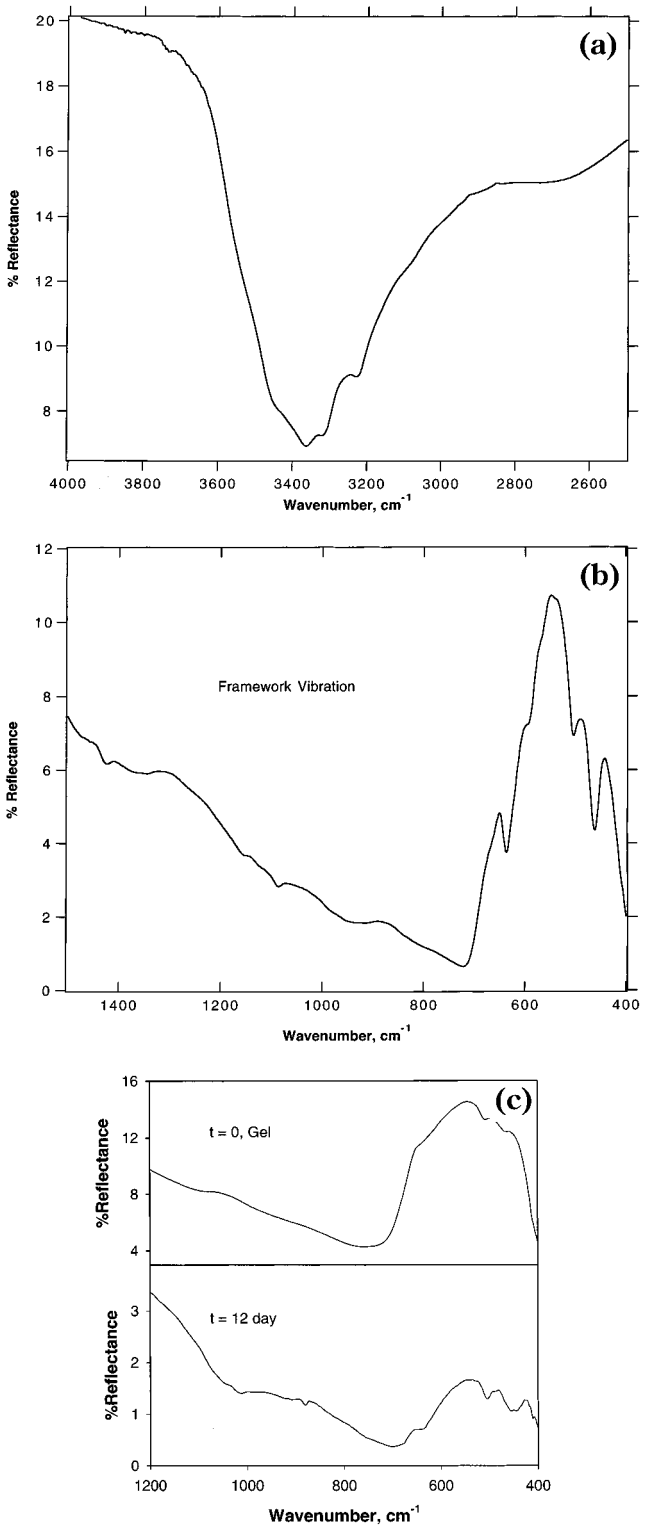

Figure 3. IR spectra of birnessites: t = 75 days, hydroxyl absorption (a); t = 75 days, framework vibration (b); and t = 0 and 12 days, framework vibration (c).

induction period and crystallization rate on temperature. The effect of temperature, basicity, and MnO_4^-/Mn^{2+} ratio were studied in syntheses using acetates. When the aging temperature was −2 °C, the crystallization of birnessite was impeded. The amount of birnessite was less than 8%, even after 30 days. When the temperature was increased from 27 to 40 °C, the induction period was shortened from 30 h to less than 10 h. The crystallization rate became faster. The phase

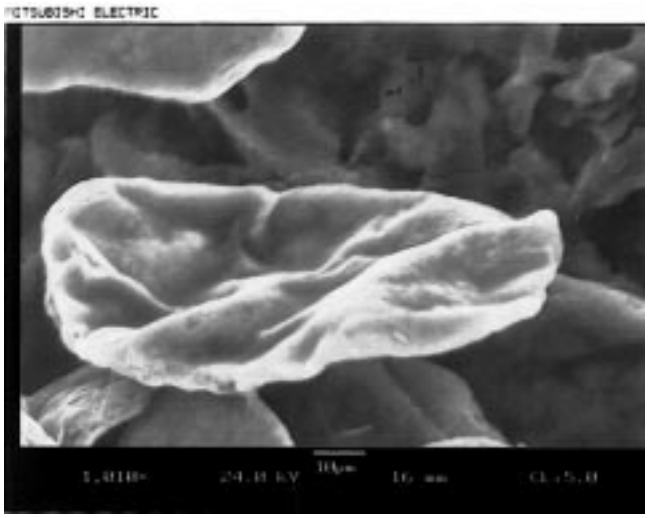

Figure 4. SEM photograph of birnessite.

Table 1. Induction Periods and Crystallization Rates of Birnessites Synthesized at Different Temperatures ($[OH^-]$ = 1.6 mol/L, MnO_4^-/Mn^{2+} = 0.4)

temp, °C	induction period	crystallization rate, h^{-1}
−2	>1 month	n/a
27	30 h	0.28
40	10−14 h	0.80
65	1−2 h	3.1
82	<1 h	7.2

Table 2. Induction Periods and Crystallization Rates of Birnessites Synthesized at Different Basicities (Room Temperature, MnO_4^-/Mn^{2+} = 0.4)

$[OH^-]$, mol/L	induction period	crystallization rate, h^{-1}
0.17	>1 week	n/a
0.64	60 h	0.049
1.6	30 h	0.28
2.6	10−12 h	1.6
3.6	8 h	3.6

transformation of feitknechtite was accelerated. At 65 °C, the crystallization started shortly after the beginning of aging. The induction period (if one existed) was less than 2 h. Almost no induction period was observed at 85 °C. The crystallization of birnessite and the phase transformation were complete in 1 day (Figure 5a−d).

Some of the basic data such as the induction period and crystallization rates are summarized in Table 2. Amorphous MnO_x was obtained for the reaction of Mn^{2+} and MnO_4^- when no NaOH was used and when an equivalent amount of NaOH to Mn^{2+} was used. In acidic solution, the amorphous MnO_x formed was gradually dissolved. Birnessite began to appear at $[OH^-]$ = 0.17 mol/L, with the amount of birnessite very small and increasing very slowly so that it was hard to distinguish the induction period and fast crystallization period. When the concentration of NaOH was decreased from 1.6 mol/L (as for the typical synthesis) to 0.74 mol/L, the induction period was increased from 30 h to over 60 h. The crystallization of birnessite became very slow, and the formation and phase transformation of feitknechtite were slowed considerably. When the amount of NaOH was increased, the induction period decreased considerably, e.g., from 30 h at 1.6 mol/L to 8 h at 3.6 mol/L. The crystallization rate and the corresponding

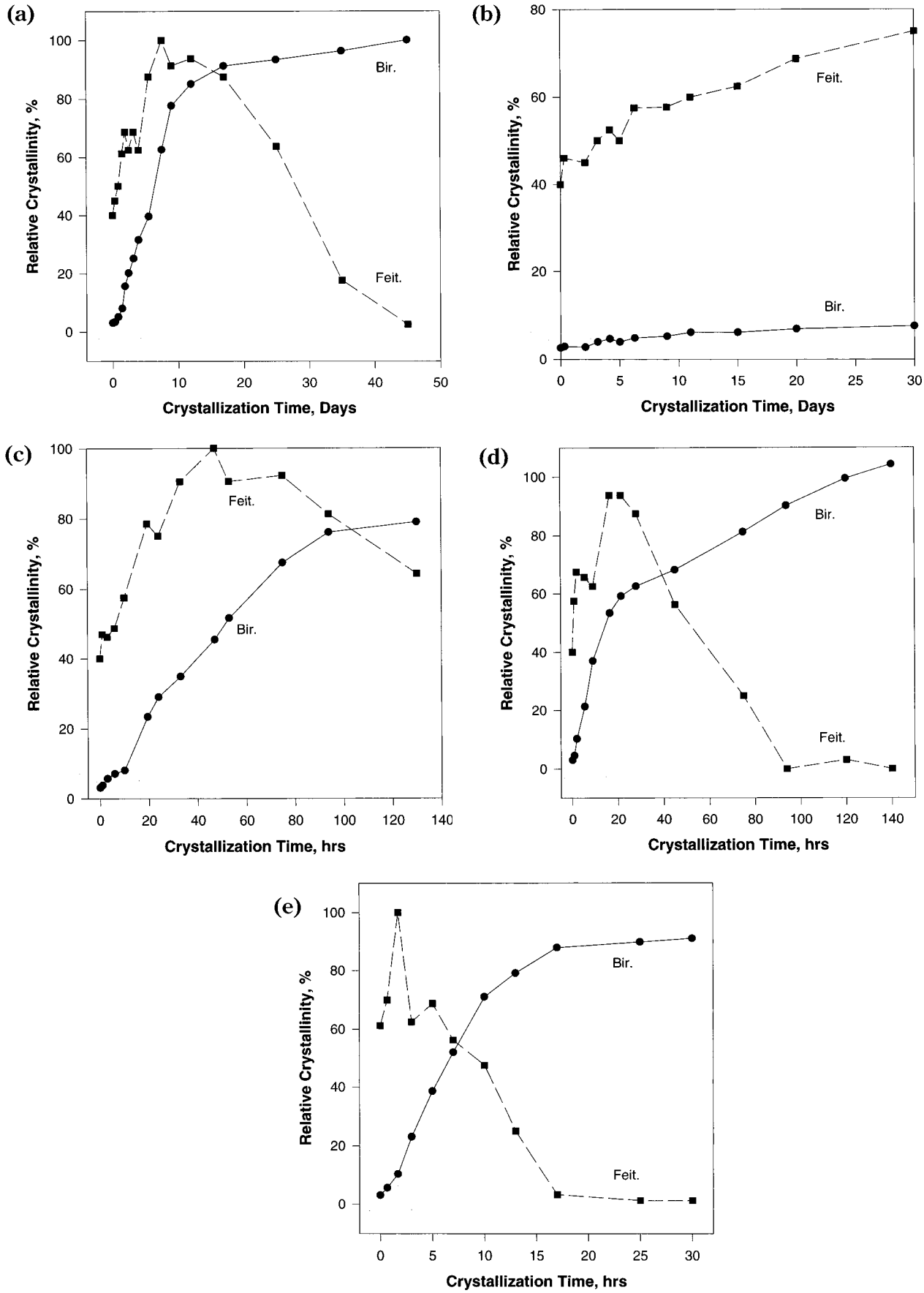

Figure 5. Crystallization curves for syntheses of birnessites at different temperatures: (a) 27 °C, (b) −2 °C, (c) 40 °C, (d) 65 °C, (e) 82 °C.

phase transformations were accelerated. The relative crystallinity of birnessite reached 100% in about 50 h.

The molar ratio of MnO_4^-/Mn^{2+} for the typical synthesis is 0.4. At a ratio of 0.17, the main products at *t*

Table 3. Induction Periods and Crystallization Rates of Birnessites Synthesized at Different MnO_4^-/Mn^{2+} Ratios (Room Temperature, $[OH^-] = 1.6$ mol/L)

MnO_4^-/Mn^{2+} ratio	induction period (h)	crystallization rate, h^{-1}
0.17	5	1.7[a]
0.21	3	2.3[a]
0.24	3	2.8[a]
0.28	2−3	n/a
0.32	1	4.0
0.36	10	1.1
0.40	30	0.28
0.46	>48	n/a

[a] Product impure, with coexistence of feitknechtite and hausmannite.

= 0 were hausmannite and feitknechtite, and no birnessite formed. Birnessite appeared at $t = 6$ h and the crystallinity increased quickly. Meanwhile, hausmannite and feitknechtite also increased with time and coexisted with birnessite for a long time. Increasing the ratio led to an increase in the amount of feitknechtite initially formed and a decrease in the amount of hausmannite initially formed. Birnessite began to form initially at $MnO_4^-/Mn^{2+} = 0.24$, with no observation of hausmannite. The amount of birnessite and feitknechtite formed initially increased on increasing the MnO_4^-/Mn^{2+} ratio until a ratio of 0.32, where they reached their maxima, when the induction period was less than 1.5 h long. At the same time, the induction period was decreased and the crystallization rate increased.

When the ratio increased above 0.32, the induction period was increased and the crystallization rate was sharply decreased. The crystallinity of feitknechtite initially formed started to decrease and then tracked the initially formed birnessite. Further increasing the ratio leads to an initial product which was almost amorphous, with an extremely long induction period and with an extremely slow crystallization rate. The amount of birnessite was less than 10% after 30 days at a ratio of 0.72. These results are summarized in Table 3 and Figure 6.

F. Phase Transformation from Buserite to Birnessite. Figure 7 shows the XRD patterns of a product (t = 60 day) exposed to air, showing that a phase transformation from buserite to birnessite had taken place. When the sample slurry was initially added to the glass slide, no peaks could be detected at this stage, where there was a large water content in the sample. With water gradually evaporating in air, the characteristic peaks of buserite began to appear and increased in intensity as the water content decreased. The peak intensities reached the highest values when the sample was just dried, at which time the characteristic peaks of birnessite began to appear while those of buserite began to decrease in intensity. Buserite peaks disappeared typically in less than 10 min at room temperature. The product was then birnessite. Obviously, the Na−buserite acts as a precursor to Na−birnessite.

The conversion from buserite to birnessite was reversible. When water was added to the dried slide, the birnessite turned back to buserite, even when the slide was heated at 50 °C for 30 min. When the slide was heated over 65 °C, the birnessite no longer changed back to buserite, even though the heated sample was immersed in water overnight. The conversion of buserite to birnessite was reported by Giovanoli et al.[33] in the formation of birnessite upon freeze-drying buserite.

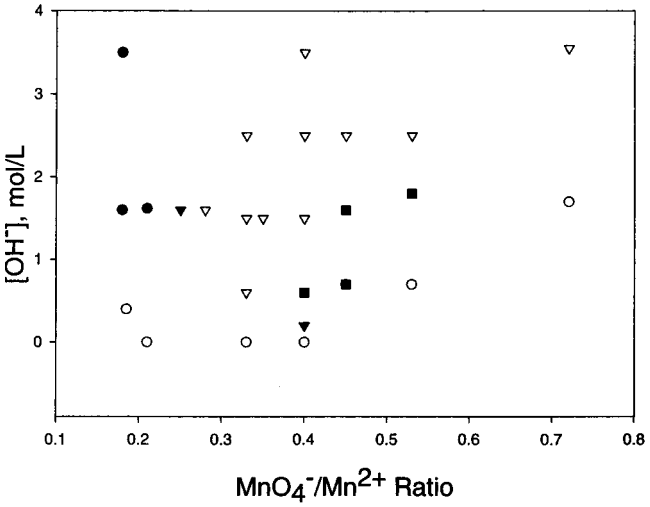

Figure 6. Phase-preparative parameters diagram for synthesis of birnessite (room temperature). (○) amorphous MnO_x, crystallinity of birnessite (if exists) less than 10%; (▽) well-crystallized birnessite; (■) birnessite in amorphous MnO_x, with crystallinity of birnessite less than 80% but greater than 50%; (▼) birnessite/feitknechtite in amorphous MnO_x, with crystallinity of birnessite usually less than 50%; (●) a mixture of birnessite, feitknechtite, and hausmannite.

IV. Discussion

A. Crystallization Process of Birnessite. The XRD peaks of birnessite at early stages (t < 5 days) are very broad and irregular. This indicates that the newly formed birnessite has very small particle size and/or a poor ordering of the layers. As the crystallization process proceeded, the particle size of birnessite increased, with a better ordering of the layers, as indicated by the narrower and symmetric XRD peaks.

Some variation in the amount of birnessite exists in this system. First, the crystal size of birnessite changed greatly during the process. When the crystal size was small, birnessite showed very low, broad XRD peaks, which made the estimation of the crystallinity difficult. Second, the disorder of the layers of birnessite and the corresponding peak irregularity also add to the difficulty in estimating the crystallinity. The preferential orientation of birnessites was consistent (the ratio of the area of the two peaks at 2θ of 12.5° (002) and 25° (212) was roughly constant for all samples; see Figures 1 and 2). The integration of peak areas was satisfactorily reproducible, with a relative deviation of <10%. When the XRD patterns are carefully made under identical conditions, the crystallinity of birnessite can be properly measured and used to describe the general trends of the crystallization process.

Figure 2 shows the crystallization curve from the XRD results. The curve exhibits three different sections. In the first section the crystallinity increases very slowly from 1% at $t = 0$ to 2% at $t = 32$ h. After that it increases rapidly and almost linearly to 82% at $t = 9$ days. The increase in crystallinity then slows down, reaching 93% at $t = 15$ days. From then on it increases extremely slowly, gradually reaching 100% over a very long period, at $t = 50$ day. Corresponding to the three sections, the crystallization of birnessite can be divided

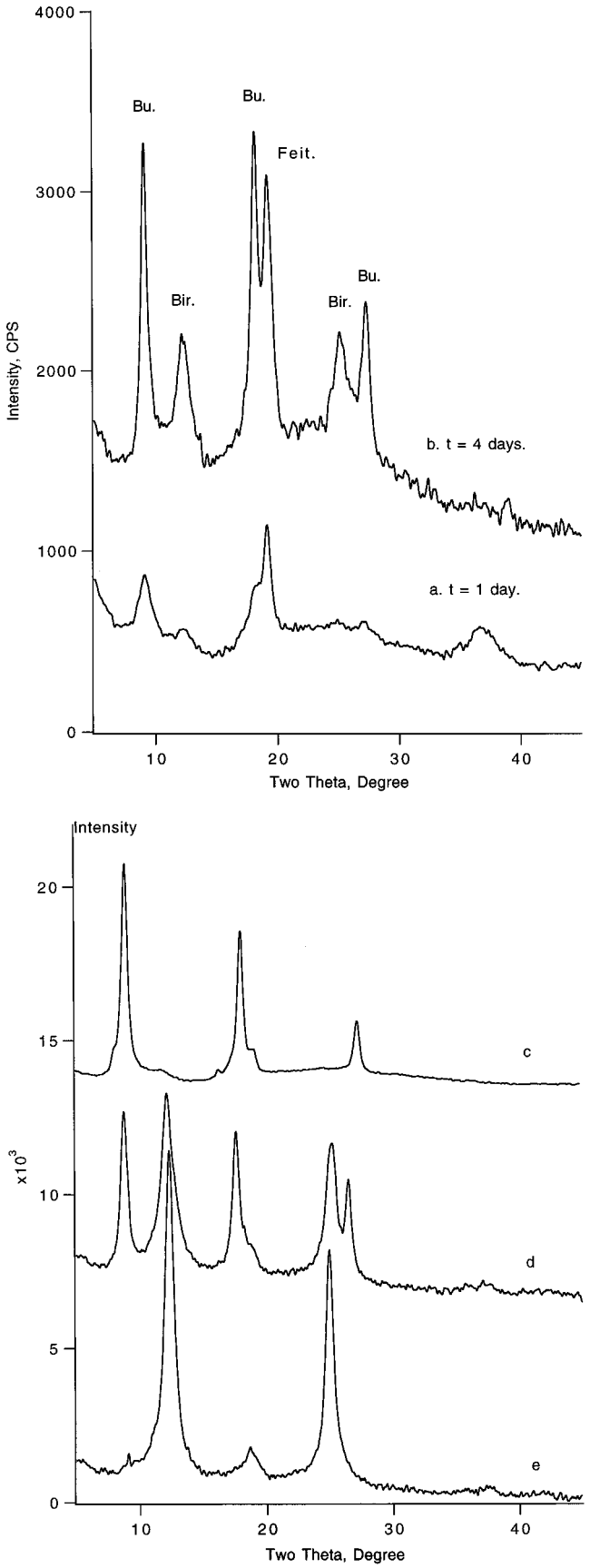

Figure 7. XRD patterns showing the conversion from buserite to birnessite A sample of $t = 1$ day (a) and 4 days (b). A sample of $t = 60$ days before (c, not fully dried), in the process of (d, newly dried), and after (e, fully dried) the conversion from buserite to birnessite due to partial dehydration.

into three stages: an induction period, a fast crystallization period, and a steady-state period. These three stages are accompanied by a period of transformation of feitknechtite. The syntheses of birnessite with acetates at 27 and 40 °C also follow these stages (See Figure 5b, 5c).

B. Phase Transformation of Feitknechtite. Feitnechtite is the main phase in the beginning. The amount of feitknechtite increased steadily during the induction period of birnessite. During the early rapid crystallization period of birnessite, the amount of feitknechtite also increased considerably, although not as fast as the amount of birnessite.

The crystallinity of feitknechtite enters a steady state from $t = 8$ to 25 days, and after that it gradually decreased and totally disappeared in $t = 75$ days (Figure 2). Since no other phase than birnessite was present as the final product, feitknechtite must have been converted to birnessite. The curve of feitknechtite also exhibits three stages: a steady-increase period ($t < 8$ day), a steady-state period, ($t = 8-25$ days), and a phase transformation period ($t > 25$ day).

C. Possible Route for the Synthesis of Birnessite. Figure 2 shows the crystallization curves of feitknechtite and birnessite. Feitknechtite reached its highest purity at a period longer than 12 days and the purity declined at $t = 25$ days. The amount of birnessite kept increasing, although very slowly after $t = 15$ days. No evidence has been observed that the purity of birnessite will decrease, even after $t = 4$ months, indicating that birnessite is a stable phase under these experimental conditions, while feitknechtite is metastable. It appears that birnessite forms with feitknechtite as an intermediate. A possible route for the synthesis may be

$$MnO_x \rightarrow \text{feitknechtite} \rightarrow \text{birnessite} \qquad (3)$$

D. Temperature Effects and Energy of Activation of Crystallization of Birnessite. *1. Temperature Effects and Kinetics of Crystallization of Birnessites.* The synthesis includes a series of reactions and of mass transfer processes. Increasing the crystallization temperature will accelerate the rates of all these steps, and therefore the whole synthesis. Figure 5a−e shows the crystallization curves for birnessite at 27, −2, 40, 65, and 82 °C. The data for −2 °C are only a segment of the crystallization curve, while the others are complete curves. The slope of the linear portion of each crystallization curve has been defined as the crystallization rate of birnessite at that temperature. Assuming that the weight of intermediate is constant during the fast crystallization period (as shown from the almost constant intensity of feitknechtite peak) and that the formation of birnessite from the intermediate is a first-order reaction, eqs 4 and 5 are obtained:

$$r = kW_{\text{int}} = \mathrm{d}W_{\text{bir}}/\mathrm{d}t \qquad (4)$$

$$\mathrm{d}W_{\text{bir}} = W\,\mathrm{d}X_{\text{bir}} \qquad (5)$$

where r is the crystallization rate of birnessite, k is the rate constant, W_{int} is the weight of intermediate, $\mathrm{d}W_{\text{bir}}$ is the weight increase of birnessite, $\mathrm{d}t$ is the time difference, $\mathrm{d}X_{\text{bir}}$ is the increase in amount of birnessite,

and W is the weight of the reaction products on a solids basis. This includes the weights of birnessite, gel, feitknechtite, etc. but does not include soluble salts. Equations 6 and 7 can then be derived as follows:

$$r = kW_{\text{int}} = W\, \mathrm{d}X_{\text{bir}}/\mathrm{d}t \tag{6}$$

$$k' = (W_{\text{int}}/W)k = \mathrm{d}X_{\text{bir}}/\mathrm{d}t \tag{7}$$

where k' is a new crystallization rate. The slope ($\mathrm{d}X_{\text{bir}}/\mathrm{d}t$) of the crystallinity−time curve is the crystalization rate at a given temperature. For each curve, five points from the linear portion were chosen to obtain a least-squares fitting to determine the crystallization rate of birnessite. The crystallization rates of birnessite obtained in this way at 27, 40, 60, and 82 °C are 0.28, 0.80, 3.1, and 7.2 h^{-1}, respectively (see Figure 5 and Table 1). The correlation coefficients for the least-squares fittings are very close to 1. This would appear to justify the assumption that the formation of birnessite is a first-order reaction.

From the data of crystallization rates (k) at different temperatures (T), an Arrhenius plot of $\ln k - 1/T$ gives an energy of activation of the crystallization of birnessite of 52 kJ/mol.

2. Basicity Effects. The crystallization rate of birnessite increases exponentially on increasing the basicity of the system. From the data in Table 2, the dependence of the crystallization rate constant on the concentration of OH^- can be obtained by using a least-squares fitting, as expressed in eq 8:

$$k = 0.12[OH^-]^{2.7} \tag{8}$$

In the above discussion, a liquid mechanism was employed to describe the synthesis of birnessite. MnO_x is an amphoteric oxide. At higher basicities, as well as at high temperatures, the solubility of the MnO_x gel will be increased. The rate of condensation reactions is also increased. The induction period is therefore decreased and the crystallization rate will be increased markedly.

3. Effects of Ratios of MnO_4^-/Mn^{2+}. At low MnO_4^-/Mn^{2+} ratios, the main initial crystalline phase is a lower valent manganese oxide, hausmannite, and then feitknechtite. Birnessite forms initially when the ratio is higher than 0.25 and its amount is increased on increasing this ratio. When the ratio is further increased (>0.32), the formation and growth of birnessite becomes more and more difficult. The starting product becomes an amorphous manganese oxide with higher manganese oxidation state. The phases present at different basicity and MnO_4^-/Mn^{2+} ratios could be summarized in a phase-preparative parameters diagram of the system (this would not be a phase diagram since the system is not really in equilibrium). Pure birnessite can be obtained in the range of MnO_4^-/Mn^{2+} ratio of 0.28−0.72 when $[OH^-]$ is greater than 1.6 mol/L. The crystallization rate is much larger when the ratio is 0.28−0.36, at which birnessite of high purity can be obtained in a short time, especially when the temperature is a little higher than room temperature, from 40 to 65 °C.

E. Buserite as a Precursor to Birnessite. In Figure 6, the peaks of buserite decrease in intensity while those of birnessite begin to appear and increase, showing that Na−buserite is an unstable phase under these conditions and is a short-lived precursor to Na−birnessite.

Birnessite and buserite are both layered materials, with one and two layers of hydrates. When the sample is still wet or just newly dried, there are enough water molecules in the layers and the sample exists in the form of the buserite structure. After the sample is dried, some of the water molecules retained in the layers begin to escape into the atmosphere, producing the less hydrated birnessite phase. If water is added to the partially dehydrated birnessite, water molecules will enter between the layers, leading to the recovery of the buserite structure.

The conversion between buserite and birnessite occurs at all stages of the crystallization. Parts a and b of Figure 7 are the XRD patterns of samples at 1 and 4 days, respectively, showing that the conversion from buserite to birnessite is underway, even though the crystallization of birnessite is in the induction period or early fast crystallization period. In Figure 7a, the broad peaks of buserite are shifting to the broad peaks of birnessite, while the peaks at 2θ of 19.5° retain their position.

V. Conclusions

The crystallization of Na−birnessite comprises three stages: an induction period, a fast crystallization period, and a steady-state period, accompanied by the formation and phase transformation of feitknechtite. Increasing the aging temperature and/or basicity will lead to reduction of the induction period, the enhancement of the crystallization rate, and the acceleration of the phase transformation of feitknechtite. Pure birnessite product can be obtained quickly when the $[OH^-]$ is greater than 1.6 mol/L at a MnO_4^-/Mn^{2+} ratio of 0.28−0.36 and at 40−65 °C. Buserite is a short-lived precursor to birnessite. The conversion from buserite to birnessite occurs at room temperature due to partial dehydration and is reversible on rehydration below 65 °C.

Acknowledgment. The authors acknowledge the support from the Office of Basic Energy Sciences, Division of Chemical Sciences of the Department of Energy. We also thank Dr. F. S. Galasso for stimulating and helpful discussions.

CM970745C